ASM GaN: Industry Standard Model for GaN RF and Power Devices—Part 1: DC, CV, and RF Model

Sourabh Khandelwal, Yogesh Singh Chauhan, Tor A. Fjeldly, *Fellow, IEEE*, Sudip Ghosh, Ahtisham Pampori, Dhawal Mahajan, Raghvendra Dangi, and Sheikh Aamir Ahsan

***Abstract*— We present the latest developments in Advance SPICE Model for GaN (ASM GaN) HEMTs in this paper. The ASM GaN model has been recently selected as an industry-standard compact model for GaN radio frequency (RF) and power devices. The core surface-potential calculation and the modeling of real device effects in this model are presented. We discuss the details of the nonlinear access region model and enhancement in this model to include a physical dependence on barrier thickness. We also present the novel model feature of configurable field-plate modeling and discuss the extraction procedure for the same. New results with the ASM GaN model on high-frequency and enhancement-mode GaN power devices are also presented.**

***Index Terms*— Advance SPICE Model for GaN (ASM GaN), compact models, GaN HEMT, SPICE model, surface potential, GaN FET.**

I. Introduction

GALLIUM nitride-based RF and power devices have gained tremendous momentum in recent years for next-generation communication [1] and power electronic applications [2]. Remarkable device properties such as high breakdown voltage, charge density, mobility, and saturation velocity increasingly enable the improved performances for both RF and power circuits. To extract the best circuit-level performance from these devices in a time and cost effective manner, advanced simulations and modeling capabilities are necessary. Indeed, GaN device modeling is a very active research area. Several compact modeling solutions have been proposed over the years with a variety of modeling methodologies. The proposed models range from table-based [3], measurement-based [4], empirical [5], neural network-based [6], behavioral model [7], threshold-voltage-based [8] to surface-potential-based models [9], [10].

The need for an accurate compact model was realized by the industry compact model standardization committee, also known as the Compact Model Coalition (CMC) [11]. CMC preferred a physics-based modeling methodology due to the following known advantages of physics-based models: physical model scalability with respect to device geometry such as channel length, physically grounded parameters, physical behavior under extreme input conditions, which may arise during circuit simulations, and predictability. CMC model standardization is a rigorous multistep process. After almost seven years of research and development, the Advance SPICE Model for GaN (ASM GaN) passed all the steps of the CMC standardization process and has been selected as an industry standard model. This paper discusses the ASM GaN model basics in brief for the benefit of readers and details the latest developments in this model. Specifically, the modeling of the nonlinear access region resistance and its multibias dependence is discussed. A new physical model to include the effect of barrier thickness on access region resistance is developed and included in the ASM GaN model. Furthermore, the novel model feature of configurable field-plate modeling, i.e., the capability to model any combination of the two different types of field plates (source-connected or gate-connected) for up to four field plates, is presented.

This paper is arranged as follows. In Section II, we briefly describe the core surface-potential calculation in the ASM GaN model. In Section III, we discuss the modeling of real device phenomena covering the ASM GaN model formulations that have not been covered in detail in our previous works. In Section IV, we present new model results for high-frequency GaN and enhancement-mode GaN power devices. In Section V, we conclude the paper.

II. Core Model

The ASM GaN model consists of a core model and the models of many real-device effects occurring in the GaN device. This model development started in [12]. The complete model can be visualized as shown in Fig. 1, which consists of a core formulation and real-device effects modeled by building on the foundation of the core surface-potential solution.

Manuscript received May 15, 2018; revised August 14, 2018; accepted August 21, 2018. Date of publication September 28, 2018; date of current version December 24, 2018. The review of this paper was arranged by Editor B. Iñiguez. *(Corresponding author: Sourabh Khandelwal.)*

S. Khandelwal and D. Mahajan are with the School of Engineering, Macquarie University, Sydney, NSW 2109, Australia (e-mail: sourabh.khandelwal@mq.edu.au).

Y. S. Chauhan, S. Ghosh, A. Pampori, R. Dangi, and S. A. Ahsan are with the Department of Electrical Engineering, IIT Kanpur, Kanpur 208016, India.

T. A. Fjeldly is with the Department of Electronics and Telecommunications, Norwegian University of Science and Technology, 7491 Trondheim, Norway.

Color versions of one or more of the figures in this paper are available online at http://ieeexplore.ieee.org.

Digital Object Identifier 10.1109/TED.2018.2867874

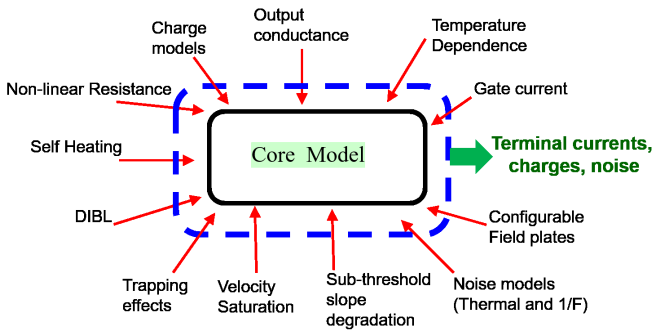

Fig. 1. ASM GaN HEMT model consists of core and models of several real-device effects in the GaN device.

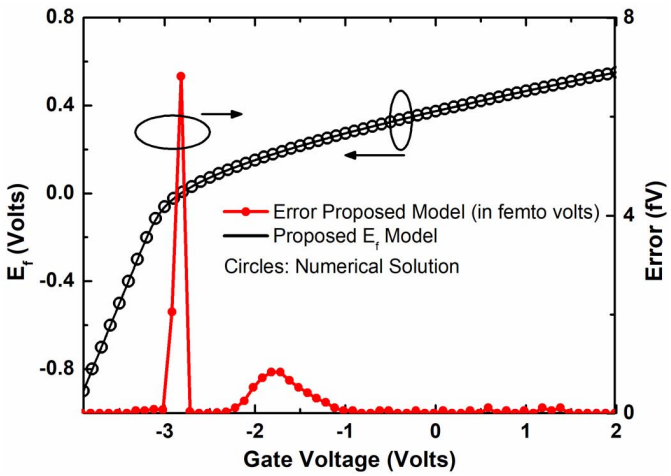

Fig. 2. Unified model for the position of the Fermi level in the quantum well of GaN HEMTs consists of the core used in the ASM GaN model.

The core model is the calculation of surface potential in the quantum well of the GaN HEMT. This has been described in our earlier works [13]–[15]. This is briefly included here for the benefit of the readers. The 2-D electron gas (2-DEG) charge in the quantum well of GaN HEMTs is a complex transcendental function of input voltages originating from Schrödinger's and Poisson's equations. In the ASM GaN model, we developed an analytical and consistent solution for these complex equations by dividing the variation of Fermi level (E_F) with input voltage into three different regions. These regions are defined based on the position of the Fermi level with respect to the energy levels in the quantum well (see [13] and [14] for more details on these regions). The analytical solutions in the different regions were then combined to yield a highly accurate and robust unified analytical solution. A comparison of the developed model with numerical simulations is shown in Fig. 2. The error plot in Fig. 2 underlines the high accuracy of the developed solution. In addition to being accurate, this solution is mathematically robust and several orders of derivatives of this analytical formulation are continuous and smooth. This is very important for a good convergence of the model in circuit simulators.

Current and charges in the GaN device are modeled by applying the drift-diffusion theory and the Ward–Dutton

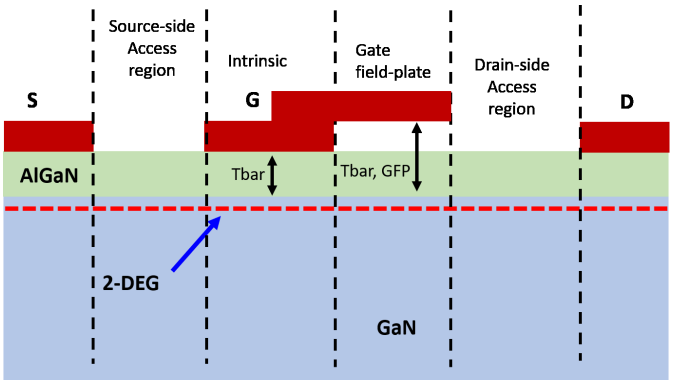

Fig. 3. Typical GaN device with gate field plate. Core surface-potential calculation performed with effective barrier layer thickness ($T_{bar,GFP}$) is to model this region of the device.

charge partitioning scheme as described in [15]. This completes the core part of the ASM GaN model.

III. Modeling of Real-Device Effects

Several real-device effects (see Fig. 1) such as velocity saturation, drain-induced barrier lowering, mobility field dependence, temperature effects, output conductance model, self-heating effect, gate leakage [16], thermal noise [17], flicker noise [18], etc., occurring in the GaN device are accounted for in the model to get an accurate model of the behavior of experimental devices. The models for these have been explained in our previous papers. Here, we describe the modeling of the nonlinear access region resistances and a model of the field-plate regions which can be configured to capture any different combination of the gate- or source-connected field plates in the GaN device.

A. Access Region Resistance Model

GaN transistors have a finite distance from the gate edge toward the source or drain to the beginning of the metallic contacts (see Fig. 3). These regions are called and the source- and drain-side access regions, respectively. The access regions behave as nonlinear resistors. The value of the resistance of the access regions depends on both the gate and drain voltages. Fig. 4 shows the value of drain-side access region resistance for varying gate and drain voltages after accurately modeling an experimental GaN HEMT device [19]. The explanation of this complex bias dependence is that the charge responsible for current flow in the access region varies negligibly with the applied gate voltage, as opposed to the region of the device under the gate where the 2-DEG charge increases by increasing the gate voltage. As the channel region charge increases, for current continuity, the charges in the access region need to travel faster and the access region behaves like a linear resistor initially. However, as these charges in the access regions reach their saturation velocity, the resistance of this region behaves nonlinearly and increases rapidly with the gate and drain voltages. This phenomenon is accurately modeled in the ASM GaN model by calculating the amount

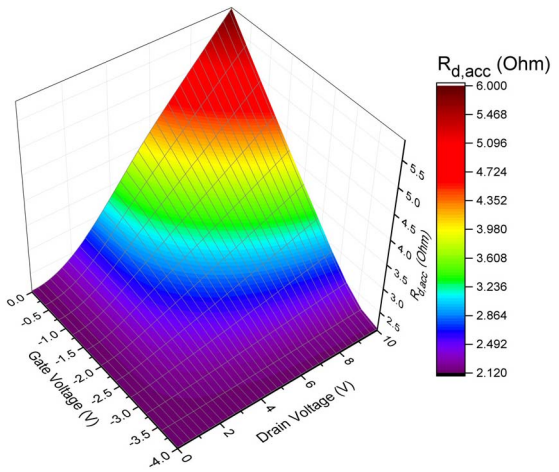

Fig. 4. Drain-side access region resistance of GaN device depends on both gate input bias and drain input bias nonlinearly. This multi-input nonlinear dependence is modeled in ASM GaN model.

of maximum current the access regions allow. This is given by

$$I_{\max} = W n_{\text{sacc}} \upsilon_{\text{sat}} \tag{1}$$

where W is the device width, n_{sacc} is the 2-DEG charge density in the access region, and υ_{sat} is the saturation velocity. Note that n_{sacc} is different than the 2-DEG charge density under that gate region as the layer structure above the 2-DEG interface in this region is different than the region under gate. The resistance of access region then becomes

$$R_{\text{acc}} = \frac{L_{\text{acc}}}{W \mu n_{\text{sacc}} (1-(I_{\text{d}}/I_{\max})^{\beta})^{1/\beta}} \tag{2}$$

where L_{acc} is the access region length, μ is the carrier mobility, I_d is the drain current, and β is a smoothening parameter with a typical value of 2. This formulation includes both the gate- and drain-voltage dependence of the access region resistance.

The 2-DEG charge density n_{sacc} controls the resistance of this region. Here, we develop a simple physical model to include the effect of a change in barrier thickness on n_{sacc}. The 2-DEG charge density n_{sacc} is partly induced by the strong piezoelectric effect in the thin AlGaN barrier layer and, if present, by dopants in the barrier (neglected here). However, a significant contribution to the 2-DEG also results from ionized surface/interface donor states at the top of the barrier layer. In particular, the effects of the surface donor states have been a persistent impediment to establishing a satisfactory physics-based understanding of how the AlGaN/GaN-based structures functions. In fact, only over the past decade or so, experimental results have shown that the density of ionized donor states is distributed over a finite energy range instead of being in a narrow spike pinned at the surface Fermi level [20], [21]. Here, we describe a model for n_{sacc} consistent with the electrostatics in this region and the experimental observations on the effect of barrier layer thickness on GaN HEMT's characteristics.

To this end, we introduce a simple box-type model for the distribution of the ionized surface donors in terms of

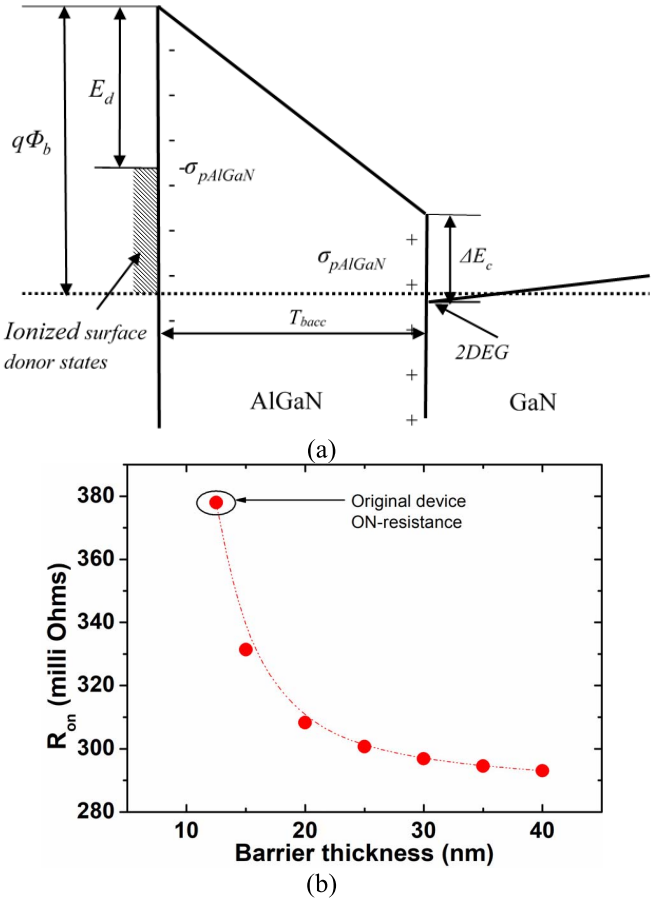

Fig. 5. (a) Energy band diagram indicating surface donor states and electrostatics in the access region for the 2-DEG charge density calculation. (b) Impact of scaling the barrier layer thickness on the on-resistance of the device.

the parameters n_o and E_d. Here, n_o is a constant ionized donor population per unit area and energy, and the donor level E_d, which defines the maximum energy of the population. As illustrated in the conduction band diagram in Fig. 5(a), E_d corresponds to the energy separation between the AlGaN surface conduction band minimum and the maximum energy for the ionized donors. Accordingly, the energy range of the ionized donors is $q\phi_b - E_d$, where $q\phi_b$ is the surface barrier height corresponding to the height of the AlGaN surface conduction-band minimum relative of the Fermi level E_F. Accordingly, the surface charge per unit area from the ionized donors is $n_o(q\phi_b - E_d)$. To relate the surface donor state properties given by the model parameters n_o and E_d to the 2-DEG charge density n_{sacc}, we impose overall charge neutrality. This requires that the surface charge per unit area from the ionized donors is equal and opposite to the 2-DEG charge density. Thus, accounting for the electrostatics across the structure, we obtain the following expressions for n_{sacc} in terms of the model parameter n_o and E_d as:

$$n_{\text{sacc}} = \frac{\sigma_{\text{pz}}(1 - d_o/T_{\text{bacc}})}{q(1 + \varepsilon_{\text{AlGaN}}/T_{\text{bacc}} n_o q^2)} \tag{3}$$

$$d_{\text{o}} = \varepsilon_{\text{AlGaN}} \frac{(E_{\text{d}} - \Delta E_{\text{c}})}{\sigma_{\text{pz}} q} \tag{4}$$

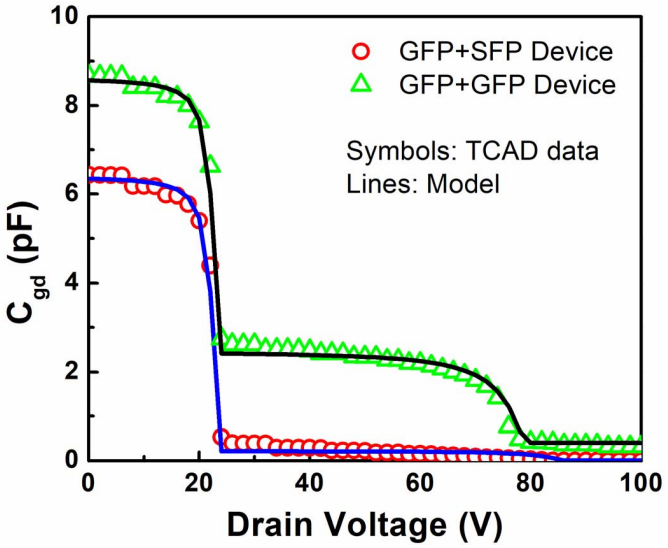

Fig. 6. Gate-to-drain capacitance of GaN power transistors modeled with ASM GaN model. Devices have different configurations of field plates. After modeling one device, the second device can be modeled by changing the FPMOD setting of the ASM GaN model.

where $\sigma_{\rm pz}$ is the positive polarization surface charge, $T_{\rm bacc}$ is the thickness of barrier layer in access region, ΔE_c is the conduction band offset at the AlGaN/GaN interface, and $\varepsilon_{\rm AlGaN}$ is the permittivity of the barrier layer. With (3) and (4) incorporated in (1) and (2), one can simulate the effect of changing barrier thickness in the access region on the device performance as shown in Fig. 5(b) and is further discussed in Section IV. This can serve as a useful tool to analyze the circuit-level impact of access region barrier thickness. Note that similar formulations have been recently presented to develop the cutoff voltage model for GaN HEMTs [22]. However, the presence of metal over the barrier will likely neutralize the trap centers partially, and a different n_o and E_d will apply in such a case. The parameters n_o and E_d introduced here can be extracted from the experimental values of $n_{\rm sacc}$ measured for the structures with varying barrier layer thicknesses.

B. Configurable Field Plate Model

In ASM GaN model, the charges of the intrinsic GaN device are modeled with the physics-based surface potential model. For the regions of the channel which are under gate- or source-connected field-plates as shown in Fig. 3, the surface-potential calculation with effective barrier layer thickness ($T_{\rm bar,GFP}$ or $T_{\rm bar,SFP}$) and appropriate cutoff voltage is performed to model the charges [23]. GaN devices can contain multiple field plates with connections to the gate or source electrode. The ASM GaN model allows modeling of all combinations of field plates possible in the device for up to four field plates via the model switch FPMOD. Setting FPMOD to 0 indicates no field plate, setting FPMOD to 1 indicates a gate-connected field plate (GFP), and setting it to 2 indicates a source-connected field plate.

In Fig. 6, we show the configurable field plate feature of the model. Fig. 6 shows gate–drain capacitance (C_{g-d}) simulations with TCAD and the ASM GaN model of a GaN device with two field plates. The first field plate in both devices is a GFP. The second field plate in device-1 (red circles in Fig. 6) is a source-connected field plate (SFP) while it is a GFP in device-2 (green triangles in Fig. 6). The height of the second field plate from the quantum well is the same in both the devices. As a result, the cutoff voltages of the second field plate region in both the devices are the same.

In the ASM GaN model, both the devices can be modeled with the setting of model field plate configurator switch named FPMOD. FPMOD can be set to GFP or SFP as needed in the device and discussed earlier. We observe different C_{g-d} in the two devices, it is interesting to note that once the device-1 capacitance has been modeled, the device-2 capacitance behavior can be accurately obtained simply by setting the FPMOD switch for the second field plate to the GFP setting. Different field plate configurations lead to considerably different capacitance as shown in Fig. 6 both of which can be accurately modeled. This underlines the accurate scalability in the model with respect to different field plate configurations. This model feature can be useful in exploring different field plate options for a targeted circuit application. For the case when $T_{\rm bar,GFP}$ and $T_{\rm bar,SFP}$ are not known, the CV behavior can serve as a very useful means to estimate these values. For instance, for the device with two GFPs, the value of C_{g-d} in Fig. 6 for $V_{\rm ds}$ approximately between 25 and 50 V is constant since the second GFP is fully turned ON. This value of C_{g-d} can be used to estimate $T_{\rm bar,GFP}$ of the second field plate. Once this is known, the value of C_{g-d} at $V_{\rm ds} = 0$ where both field plates are fully on (while $V_{\rm gs} < V_{\rm off}$ of the main transistor) can be used to estimate the $T_{\rm bar,GFP}$ of the first field plate. Similar reasoning can be used to estimate $T_{\rm bar,SFP}$ from the measured $C_{\rm ds}$ data.

IV. Model Results

A. GaN Power Device Results

With the ASM GaN model, for the first time, we present the results for an enhancement-mode GaN device. We model the transfer and output characteristics of an enhancement-mode GaN-on-silicon device with channel length of 0.8 μm, channel width of 36 mm, source access region 0.75 μm, and drain access region length of 6 μm [24]. The enhancement-mode GaN devices have a p-GaN layer to make the cut-off voltage positive. This is needed for fail-safe operation in power electronic systems. The presence of the p-GaN layer shifts the cutoff voltage. Nevertheless, the 2-DEG formation in the quantum well follows the device physics captured by ASM GaN model. This is validated by the reasonable model results shown in Fig. 7(a) and (b) for transfer and output characteristics of this device. With the new model for the access region presented in this paper, which relates the access region 2-DEG charge density to the barrier thickness, it becomes possible to see the impact of the barrier layer thickness in the access region on I–V characteristics of the device. This model feature can be used for technology optimization. Fig. 5 (b) shows the variation on ON-resistance of this device as the barrier layer

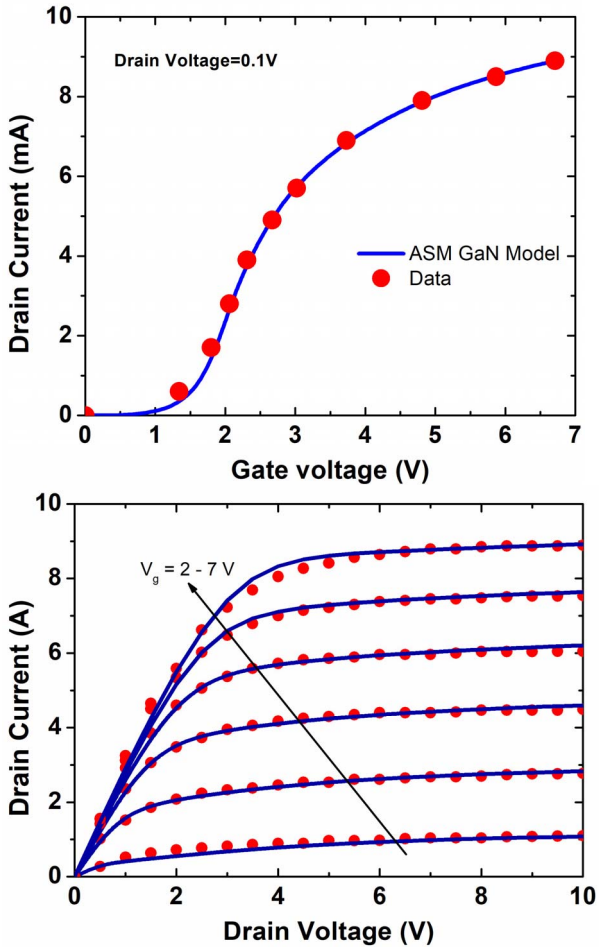

Fig. 7. Accurate modeling of (a) transfer characteristics and (b) output characteristics of an enhancement-mode GaN power device with the ASM GaN model. Experimental data are taken from [24].

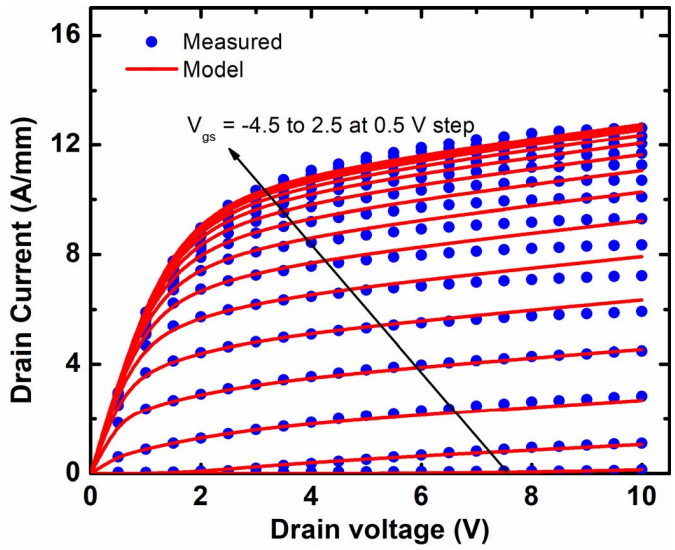

Fig. 8. Accurate modeling of dc output characteristics of aggressively scaled channel length $L = 90$ nm device with ASM GaN model. Experimental data are taken from [25].

thickness of the access region is varied. An increase of the barrier thickness in the access regions decreases the access region resistances as it increases the 2-DEG charge density.

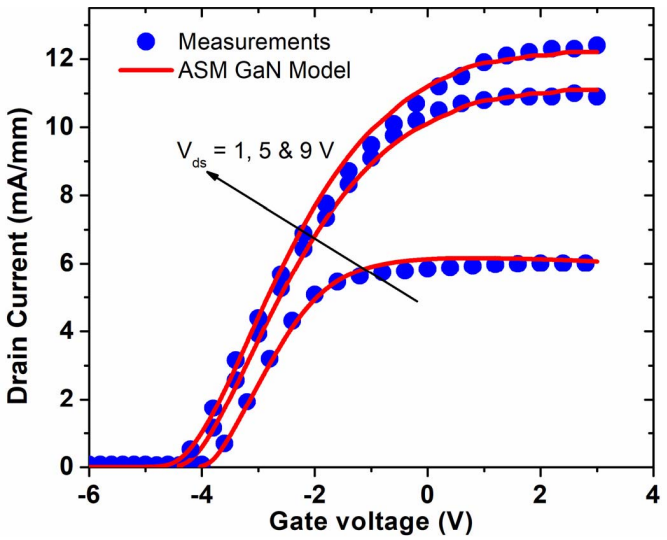

Fig. 9. Accurate modeling of dc transfer characteristics of $L = 90$ nm device with ASM GaN model. Experimental data are taken from [25].

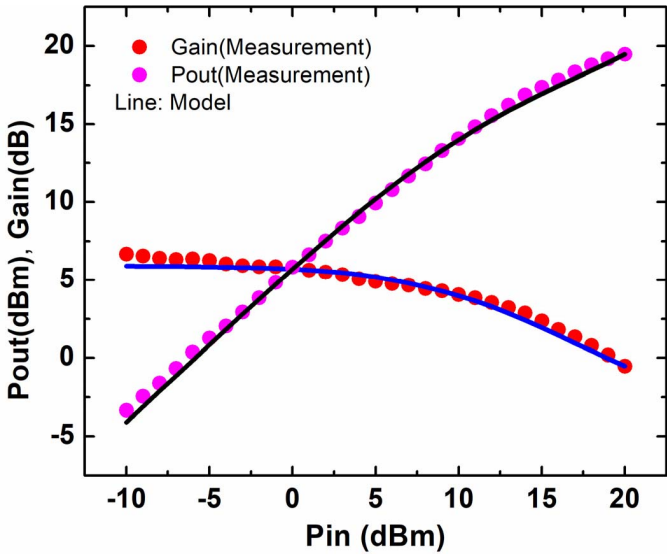

Fig. 10. Accurate modeling of large signal RF characteristics of aggressively scaled channel length $L = 160$ nm GaN HEMT with ASM GaN model. Experimental data are taken from [25].

The upper limit for barrier layer thickness will be governed by strain relaxation in the barrier layer.

B. GaN RF Device Results

GaN technology is moving rapidly, and recently, promising device characteristics for aggressively scaled channel length $L = 90$ nm device have been presented [25]. Here, we show that the current ASM GaN model can model such advanced GaN devices accurately, as shown in Figs. 8 and 9. DC output and transfer characteristics have been modeled following the extraction procedure presented in [19]. Large signal RF data at 35 GHz and $V_{ds} = 20$ V for an $L = 160$ nm device were also presented in [25]. In Fig. 10, we show that the RF characteristics of such an advanced GaN device can be accurately modeled with the ASM GaN model following the RF extraction flow discussed in [19] and [26]. Furthermore, using the developed access region resistance model discussed in Section III-A, we simulate the impact of variation in access

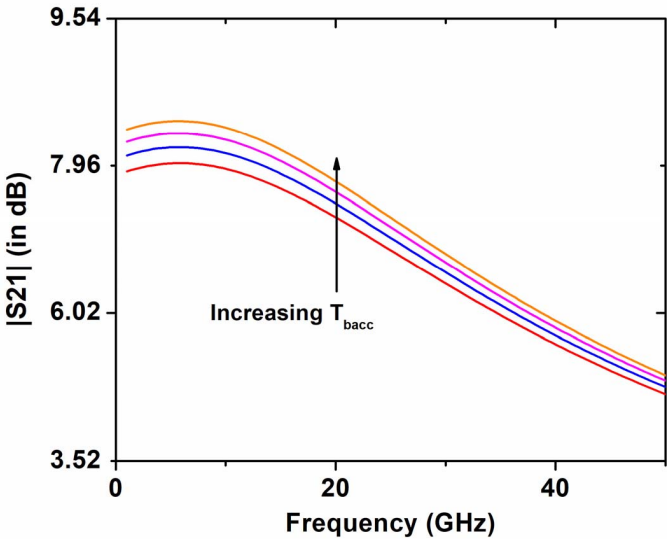

Fig. 11. Change in $|S21|$ as the barrier thickness is varied. The effect of barrier thickness is modeled with the formulations presented in Section III.

region resistance due to the increasing barrier thickness. This is shown for $S21$ in Fig. 11. As discussed in Section III, a thicker barrier reduces the access region resistance, in turn, increasing $S21$.

V. Conclusion

Recently selected industry standard ASM GaN model has been presented. Accurate model results for aggressively scaled RF and enhancement-mode GaN power devices have been achieved with this publicly available model [27], [28]. The dependence of access region 2-DEG charge density on barrier thickness has been incorporated in the model, making it a useful tool for device/circuit cooptimization. The presented configurable modeling of field plates in ASM GaN model can be used for appropriate tuning of field plates for targeted circuit application.

References

[1] J. J. Komiak, "GaN HEMT: Dominant force in high-frequency solid-state power amplifiers," *IEEE Microw. Mag.*, vol. 16, no. 3, pp. 97–105, Apr. 2015.
[2] E. A. Jones, F. F. Wang, and D. Costinett, "Review of commercial GaN power devices and GaN-based converter design challenges," *IEEE J. Emerg. Sel. Topics Power Electron.*, vol. 4, no. 3, pp. 707–719, Sep. 2016.
[3] Y. Long, Y.-X. Guo, and Z. Zhong, "A 3-D table-based method for non-quasi-static microwave FET devices modeling," *IEEE Trans. Microw. Theory Techn.*, vol. 60, no. 10, pp. 3088–3095, Oct. 2012.
[4] J. G. Leckey, "A scalable X-parameter model for GaAs and GaN FETs," in *Proc. Microw. Integr. Circuits Conf. (EuMIC)*, Oct. 2011, pp. 13–16.
[5] I. Angelov, H. Zirath, and N. Rorsman, "A new empirical nonlinear model for HEMT and MESFET devices," *IEEE Trans. Microw. Theory Techn.*, vol. 40, no. 12, pp. 2258–2266, Dec. 1992.
[6] J. Xu, R. Jones, S. A. Harris, T. Nielsen, and D. E. Root, "Dynamic FET model-DynaFET-for GaN transistors from NVNA active source injection measurements," in *IEEE MTT-S Int. Microw. Symp. Dig.*, Jun. 2014, pp. 1–3.
[7] A. Raffo, G. Bosi, V. Vadalá, and G. Vannini, "Behavioral modeling of GaN FETs: A load-line approach," *IEEE Trans. Microw. Theory Techn.*, vol. 62, no. 1, pp. 73–82, Jan. 2014.
[8] U. Radhakrishna, T. Imada, T. Palacios, and D. Antoniadis, "MIT virtual source GaNFET-high voltage (MVSG-HV) model: A physics based compact model for HV-GaN HEMTs," *Phys. Status Solidi C*, vol. 11, nos. 3–4, pp. 848–852, Mar. 2014.
[9] S. Khandelwal *et al.*, "Robust surface-potential-based compact model for GaN HEMT IC design," *IEEE Trans. Electron Devices*, vol. 60, no. 10, pp. 3216–3222, Oct. 2013.
[10] P. Martin and L. Lucci, "A compact model of AlGaN/GaN HEMTs power transistors based on a surface-potential approach," in *Proc. 20th Int. Conf. Mixed Design Integr. Circuits Syst.*, Jun. 2013, pp. 92–95.
[11] Accessed: Mar. 15, 2018. [Online]. Available: http://www.si2.org/cmc/
[12] S. Khandelwal, "Compact modeling solutions for advanced semiconductor devices," Ph.D. dissertation, Dept. Electron. Telecommun., Norwegian Univ. Sci. Technol., Trondheim, Norway, Sep. 2013.
[13] S. Khandelwal, N. Goyal, and T. A. Fjeldly, "A physics-based analytical model for 2DEG charge density in AlGaN/GaN HEMT devices," *IEEE Trans. Electron Devices*, vol. 58, no. 10, pp. 3622–3625, Oct. 2011.
[14] S. Khandelwal and T. A. Fjeldly, "A physics based compact model of I–V and C–V characteristics in AlGaN/GaN HEMT devices," *Solid-State Electron.*, vol. 76, pp. 60–66, Oct. 2012.
[15] S. Khandelwal, Y. S. Chauhan, and T. A. Fjeldly, "Analytical modeling of surface-potential and intrinsic charges in AlGaN/GaN HEMT devices," *IEEE Trans. Electron Devices*, vol. 59, no. 10, pp. 2856–2860, Oct. 2012.
[16] S. Ghosh, A. Dasgupta, S. Khandelwal, S. Agnihotri, and Y. S. Chauhan, "Surface-potential-based compact modeling of gate current in AlGaN/GaN HEMTs," *IEEE Trans. Electron Devices*, vol. 62, no. 2, pp. 443–448, Feb. 2015.
[17] A. Dasgupta, S. Khandelwal, and Y. S. Chauhan, "Surface potential based modeling of thermal noise for HEMT circuit simulation," *IEEE Microw. Wireless Compon. Lett.*, vol. 25, no. 6, pp. 376–378, Jun. 2015.
[18] A. Dasgupta, S. Khandelwal, and Y. S. Chauhan, "Compact modeling of flicker noise in HEMTs," *IEEE J. Electron Devices Soc.*, vol. 2, no. 6, pp. 174–178, Aug. 2014.
[19] S. Khandelwal, S. Ghosh, Y. S. Chauhan, B. Iniguez, and T. A. Fjeldly, "Surface-potential-based RF large signal model for gallium nitride HEMTs," in *Proc. IEEE Compound Semiconductor Integr. Circuit Symp. (CSICS)*, Oct. 2015, 2015.
[20] G. Koley and M. G. Spencer, "On the origin of the two-dimensional electron gas at the AlGaN/GaN heterostructure interface," *Appl. Phys. Lett.*, vol. 86, no. 4, p. 042107, 2005.
[21] N. Goyal and T. A. Fjeldly, "Surface donor states distribution post SiN passivation of AlGaN/GaN heterostructures," *Appl. Phys. Lett.*, vol. 105, no. 3, p. 033511, 2014.
[22] W. E. Muhea, F. M. Yigletu, R. Cabré-Rodon, and B. Iñiguez, "Analytical model for Schottky barrier height and threshold voltage of AlGaN/GaN HEMTs with piezoelectric effect," *IEEE Trans. Electron Devices*, vol. 65, no. 3, pp. 901–907, Mar. 2018.
[23] S. A. Ahsan, S. Ghosh, S. Khandelwal, and Y. S. Chauhan, "Analysis and modeling of cross-coupling and substrate capacitances in GaN HEMTs for power-electronic applications," *IEEE Trans. Electron Devices*, vol. 64, no. 3, pp. 816–823, Mar. 2017.
[24] X. Li, M. Van Hove, M. Zhao, K. Geens, V.-P. Lempinen, and J. Sormunen, "200 V enhancement-mode p-GaN HEMTs fabricated on 200 mm GaN-on-SoI with trench isolation for monolithic integration," *IEEE Electron Device Lett.*, vol. 38, no. 7, pp. 918–921, Jul. 2017.
[25] H. Zhou *et al.*, "DC and RF performance of AlGaN/GaN/SiC MOSHEMTs with deep sub-micron T-gates and atomic layer epitaxy MgCaO as gate dielectric," *IEEE Electron Device Lett.*, vol. 38, no. 10, pp. 1409–1412, Oct. 2017.
[26] S. Aamir Ahsan, S. Ghosh, S. Khandelwal, and Y. S. Chauhan, "Physics-based multi-bias RF large-signal GaN HEMT modeling and parameter extraction flow," *IEEE J. Electron Devices Soc.*, vol. 5, no. 5, pp. 310–319, Sep. 2017.
[27] Accessed: Mar. 15, 2018. [Online]. Available: https://research.science.mq.edu.au/edac/
[28] Accessed: Mar. 15, 2018. [Online]. Available: http://iitk.ac.in/asm/

Sourabh Khandelwal is a Senior Lecturer with Macquarie University, Sydney, NSW, Australia. He is the Lead Developer of the ASM-HEMT Compact Model. He has published over 90 research publications on semiconductor devices.

Mr. Khandelwal is an Associate Editor of the IEEE Access.

Yogesh Singh Chauhan is an Associate Professor with IIT Kanpur, Kanpur, India. He is the Developer of industry standard BSIM-BULK (formerly BSIM6) model for bulk MOSFETs and ASM-HEMT model for GaN HEMTs.

Mr. Chauhan is the Editor of the IEEE Transactions on Electron Devices and a Distinguished Lecturer of the IEEE Electron Devices Society.

Tor A. Fjeldly (M'85–SM'88–F'00) is an Emeritus Professor at the Norwegian University of Science and Technology, Trondheim, Norway. He has published over 250 scientific and technical works including 10 books (co-edited and/or co-authored) and 17 book chapters, in addition to papers in international journals and conference proceedings.

Sudip Ghosh received the Ph.D. degree from the University of Bordeaux 1, Bordeaux, France, in 2012, and the M.Sc. degree from Jadavpur University, Kolkata, India, in 2008.

He was a Guest Researcher with the Department of Energy Technology, Aalborg University, Aalborg, Denmark, in 2013. He is currently a SERB Young Scientist with IIT Kanpur, Kanpur, India.

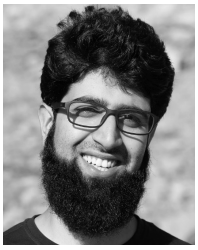

Ahtisham Pampori received the B.Tech. degree in electronics and communications engineering from the National Institute of Technology, Srinagar, India, in 2015.

He served as an Associate Consultant at Frost & Sullivan Sdn. Bhd., Kuala Lumpur, Malaysia, before joining IIT Kanpur, Kanpur, India, for his Ph.D. in 2017. His current research interests include AlGaN/GaN-based devices-their characterization, modeling, and deployment in RF circuits.

Dhawal Mahajan is currently pursuing the Ph.D. degree with Macquarie University, Sydney, NSW, Australia.

He was a Modeling Engineer with Maxim Integrated, Bengaluru, India, and Globalfoundries, Bengaluru. His current research interests include semiconductor device modeling and circuit design.

Raghvendra Dangi received the B.Tech. degree from the Institute of Engineering and Technology, DAVV, Indore, India, in 2014, and the master's degree in VLSI design from the Visvesvaraya National Institute of Technology, Nagpur, India, in 2016.

As a Research Scholar at IIT Kanpur, Kanpur, India, he is primarily focused on GaN-based devices, especially trap related phenomena, their modeling and simulation.

Sheikh Aamir Ahsan, biography and photograph not available at the time of publication.